

# Surface flux pinning in superconducting amorphous $(\text{Mo}_{0.6}\text{Ru}_{0.4})\text{B}_{18}$

B. M. Clemens and W. L. Johnson

*W. M. Keck Laboratory of Engineering Materials, California Institute of Technology, Pasadena, California 91125*

(Received 19 April 1982; accepted for publication 20 July 1982)

Superconducting critical current density was measured as a function of a perpendicular applied magnetic field in glassy  $(\text{Mo}_{0.6}\text{Ru}_{0.4})_{82}\text{B}_{18}$ . The pinning force density was observed to depend linearly on  $1/w$ , where  $w$  is the sample width measured perpendicular to both the current and field. This dependence is attributed to pinning by the sample edges. The bulk pinning contribution can be separated from the edge pinning contribution by extrapolation of the  $F_p$  vs  $1/w$  curve. The edge contribution of the flux pinning was nearly eliminated by electrolytically polishing the sample. The contribution of the flux pinning profile due to edge pinning is analyzed in terms of the dynamic pinning model modified for edge pinning.

PACS numbers: 74.60.Ge, 74.60.Jg, 74.70.Lp

Critical current density has been found to be a parameter which is sensitive to the structural state of superconducting materials.<sup>1-3</sup> Evidence for defects and inhomogeneities<sup>4-6</sup> in the structure of amorphous alloys can be obtained from the study of flux pinning.<sup>2,3</sup> In amorphous materials, spatial modulation of the superconducting properties by inhomogeneities and defects on a scale comparable to the superconducting coherence length tends to be small. Thus flux pinning tends to be rather weak compared to that observed in crystalline materials. Consequently, effects such as sample edge pinning can play a very important role in the measured critical current density.

We have measured the critical current density in amorphous  $(\text{Mo}_{0.6}\text{Ru}_{0.4})_{82}\text{B}_{18}$  and found that flux pinning by the edge of the sample can account for a significant part of the observed critical current. This contribution must be taken into account if a meaningful analysis of flux pinning is to be achieved.

The samples were prepared from ingots which were induction melted in a gettered argon atmosphere. The samples were then splat cooled by the piston and anvil technique described elsewhere.<sup>7</sup> The amorphous nature of the specimens was determined by step scanning on an x-ray diffractometer using Cu  $K\alpha$  radiation. The spectra exhibited the broad smooth bands characteristic of amorphous materials. No evidence of crystallinity was observed in the samples used in this study.

Several strips of varying widths were cut from the same foil with a wire saw. The sample widths were measured with an optical micrometer. The widths ranged from about 0.1 mm to 4 mm. The sample thicknesses were about 40–50  $\mu\text{m}$ .

Critical currents were measured with a dc method using a 4 point probe. The current contacts were soldered to electroplated copper and the voltage contacts were spot-welded Pt wires. A 1- $\mu\text{V}$  potential along the sample ( $\sim 3\mu\text{V}/\text{cm}$ ) was taken as the critical current criteria. All critical current measurements were performed with the sample submerged in a liquid He<sup>4</sup> bath. A NbTi superconducting solenoid was used to produce magnetic fields up to 80 kG. The field was applied perpendicular to the current. The sample width  $w$  is defined as the dimension of the sample perpendicular to both current and field. Upper critical field and critical temperatures of the

sample were measured with the sample sealed in a chamber which contained an He exchange gas. The temperatures were measured with a carbon resistance thermometer to an absolute accuracy of 0.1 K, and a relative accuracy of 0.03 K.

The pinning force density ( $F_p$ ) is the total force per unit volume being exerted on the flux line lattice (F.L.L.) by the pinning centers. When the current density is equal to the critical current density ( $J_c$ ), the pinning force density is equal to the Lorentz Force on the F.L.L. Thus  $F_p = J_c \times B$ , where  $B$  is the magnetic field.

If pinning is done primarily by the edges of the sample, the flux lines will move unhindered through the bulk of the sample. The volume fraction of strong pinning material will be  $2d/w$ , where  $d$  is the width of the sample region where pinning occurs.

Figure 1 shows a plot of  $F_p$  versus field for several samples with different widths. The widest samples has the smallest  $F_p$ . The inset of Fig. 1 shows a plot of  $F_p$  vs  $1/w$  for several fields. The linear dependence indicates the presence

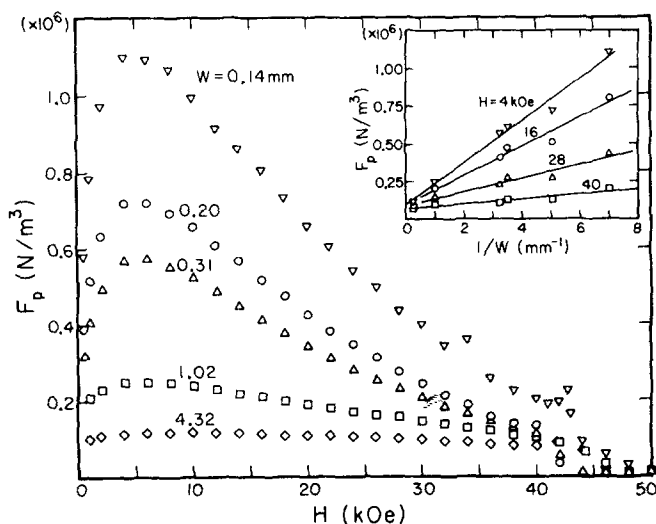


FIG. 1. Pinning force vs field for several samples with different widths (dimension of sample measured perpendicular to both current and field). Inset shows linear dependence of pinning force on  $1/w$ .

of edge pinning. The slope of  $F_p$  vs  $1/w$  is the force per unit area, or pinning pressure, on the edge of the sample. Figure 2 is a plot of the pinning pressure versus field found from a least squares fit of  $F_p$  vs  $1/w$  for each value of the field. This pinning pressure profile is very similar to the published pinning forces profiles for metallic glasses.<sup>2,8</sup> This suggests that edge pinning was present in these cases also.

The intercept of the  $F_p$  vs  $1/w$  plot gives the bulk pinning contribution of  $F_p$ . The pinning force profile obtained in this manner has no peak at low field and the pinning forces are very weak ( $\sim 5 \times 10^4$  N/m<sup>3</sup>). This extrapolation method, or an ac technique<sup>9</sup> which can separate out the surface pinning contribution, must be used if one is to obtain structural information regarding the bulk material from pinning studies.

Changes in the critical field ( $H_{c2}$ ) of the sample will of course affect the critical current. By measuring the critical current and critical field as a function of temperature, we have found that the bulk pinning force density follows a scaling relation of the form

$$F_p = Kf(h)(H_{c2})^n,$$

with  $n \approx 2$  in cases studied here. Thus the critical parameter in evaluating structural changes and their flux pinning characteristics is  $F_p/H_{c2}^2$ .

In order to gain further insight into the nature of the observed pinning force, the samples were electropolished. This treatment removed roughness and irregularities from the edges of the samples. The critical current was dramatically reduced by this treatment. Figure 3 shows  $F_p$  before and after polishing for the narrowest ( $w = 0.14$  mm) sample. This sample showed the largest decrease in pinning force upon polishing. The inset shows  $F_p$  vs  $1/w$  at an applied field of 16 kG before and after electropolishing. Note the slope is decreased by over an order of magnitude while the intercept is not altered, thus removal of surface irregularities reduced edge pinning, and we conclude that surface roughness is the

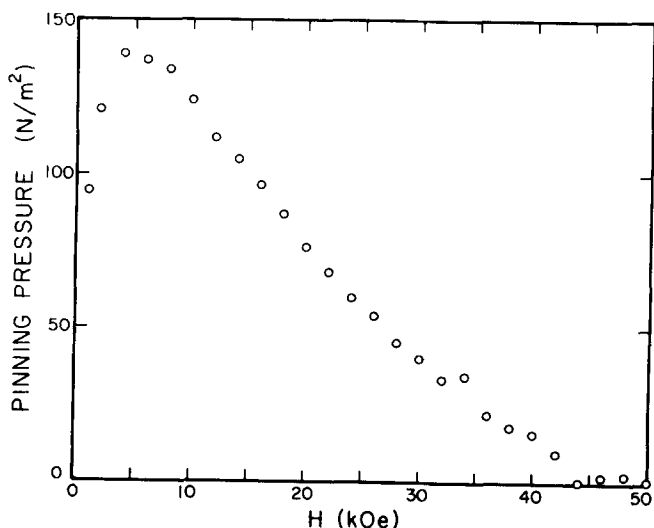


FIG. 2. The slope of pinning force vs  $1/\text{width}$  (pinning pressure) as a function of field obtained from a least square fit of pinning force vs  $1/\text{width}$  for each value of the field.

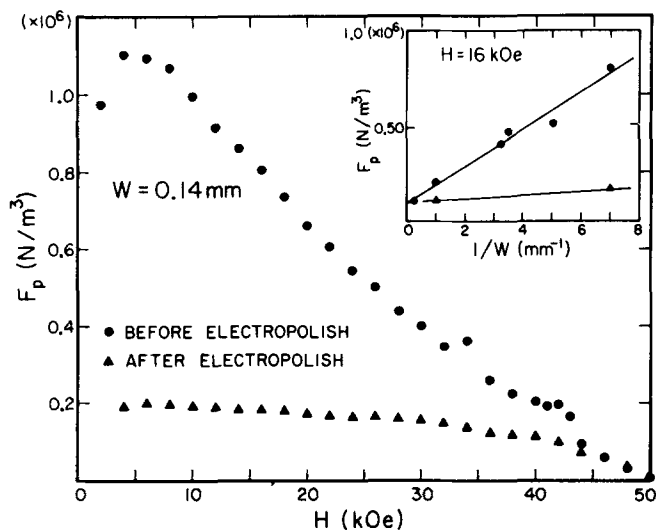


FIG. 3. Pinning force as a function of field for the narrowest ( $w = 0.14$  mm) sample. Inset shows pinning force as a function of  $1/\text{width}$  at an applied field of 16 kG before and after electropolishing.

edge pinning mechanism.

Pinning by roughness on the surfaces perpendicular to the magnetic field would produce an increase in pinning force density which is independent of the sample width. Since we observed no change in the intercept of  $F_p$  vs  $1/w$  after electropolishing the sample, we conclude that roughness on surfaces perpendicular to the magnetic field is not effective in pinning flux.

The task of computing the magnetic field dependence of the observed pinning force density  $F_p$  can be broken into two parts. First, we must determine the nature and field dependence of the force ( $f_p$ ) between an individual flux line and a defect. The second part consists in summing the forces on individual flux lines over the entire flux line lattice in a manner which takes into account the flux line-flux line interaction and the statistical nature of the pinning forces. Several authors<sup>9-11</sup> have addressed the first question and the exact form for  $f_p$  depends upon the shape of the pinning centers. In the case of point pinning  $f_p \propto (1-h)$  where as in line and plane pinning the number of vortices which can be pinned by a given pinning center is inversely proportional to the flux line lattice constant  $a_0$  giving  $f_p \propto h^{1/2}(1-h)$ . This form has recently been verified in amorphous materials.<sup>12</sup>

The summation problem has been approached from a dynamic<sup>1,13</sup> or statistical<sup>14</sup> summation or from a collective pinning approach.<sup>12,15</sup> In the dynamic pinning model<sup>1,13</sup> the energy dissipated is  $F_p \langle V_S \rangle$ , where  $\langle V_S \rangle$  is the average flux line velocity. This equal to  $E_S \langle V_S \rangle / a_0$ , where  $E_S$  is the energy of a static flux line-pinning center interaction and  $\langle V_S \rangle / a_0$  is the plucking frequency or the rate that a given pinning center interacts with the lines of the flux line lattice. In a Hooke's law approximation, the static energy of interaction is  $f_p^2 / 2c$ , where  $c$  is the effective elastic constant for the flux line lattice. This gives  $F_p = f_p^2 / 2ca_0$ . Labusch's statistical approach<sup>14</sup> yields a similar result.

Within the framework of the model discussed, the problem becomes one of determining the proper effective modulus. Labusch<sup>14</sup> has shown that the effective modulus is given

by

$$C = \left[ \frac{1}{(C_{44}C_{11})^{1/2}} + \frac{1}{(C_{44}C_{66})^{1/2}} \right]^{-1},$$

but since  $C_{66} \ll C_{11}$ ,  $C \approx (C_{44}C_{66})^{1/2}$ . Pearl<sup>16</sup> has shown that in the region near the surface, the flux line-flux line interaction goes as  $1/r$  at long distances as compared with the exponentially decreasing interaction in the bulk. This tends to increase the compressibility and decrease the shear modulus of the flux line lattice. This decrease in the shear modulus led Kramer and Das Gupta<sup>17</sup> and Das Gupta and Kramer<sup>18</sup> to postulate that the elastic energy of deformation of a flux line lattice is dominated by the bending modulus  $C_{44}$ .

The dominant feature of the flux pinning profile (Fig. 2) is the peak in  $F_p$  as a function of  $h$  which occurs at very low  $h$ . If we take  $C_{44}$  as the effective modulus, we have a pinning force density which diverges at low  $h$  since Brandt<sup>19</sup> has shown  $C_{44} \propto B^2$ . If we take  $(C_{44}C_{66})^{1/2}$  as the effective modulus and use  $f_p \propto 1 - h$  as in point defect pinning, then we also have  $F_p$  diverge as  $h \rightarrow 0$  [ $C_{66} \propto b(1 - b)^2$ ]. Obviously the measured pinning force cannot become infinite. Kramer<sup>2</sup> has suggested that when pins become very strong, the lattice shears around the strongly pinned lines. This leads to a sharp peak in the pinning profile which can be rounded off by assuming a distribution of pinning strengths. Pinning profiles generated using this type of model are found to be in good agreement with the observed pinning profile due to surface pinning. More information is needed concerning the distribution of pinning strengths to determine the actual effective elastic modulus.

In amorphous superconducting materials where flux pinning is weak, care must be taken in interpretation of critical current measurements. Surface pinning has been shown to dominate the flux pinning profile of this material and must be eliminated for critical current measurements to

yield information on the bulk structure. Once these precautions have been taken, critical current can prove to be sensitive to the structural state of metallic glasses. For instance, measurements<sup>20</sup> on annealed samples of glasses  $(\text{Mo}_{0.6}\text{Ru}_{0.4})_{82}\text{B}_{18}$  indicate that the parameter  $F_p/H_c2^2$  remains unchanged by a two-hour anneal at 450 °C and is increased by roughly a factor of two after an anneal at 550 °C for the same time. These and other data will be discussed in a separate publication.

This research was supported by the DOE under Project Agreement No. DE-AT03-81ER10870, Contract No. DE-AM03-76SF00767.

<sup>1</sup>E. J. Kramer, *J. Appl. Phys.* **44**, 1360 (1973).

<sup>2</sup>C. Koch, J. O. Scarbrough, D. M. Kroeger, and A. Das Gupta, *Appl. Phys. Lett.* **37**, 451 (1980).

<sup>3</sup>B. M. Clemens, W. L. Johnson, and J. Bennett, *J. Appl. Phys.* **51**, 1116 (1980).

<sup>4</sup>B. M. Clemens, M. Tenhover, and W. L. Johnson, *Physica* **107 B**, 319 (1981).

<sup>5</sup>C. O. Kim and W. L. Johnson, *Phys. Rev. B* **23**, 143 (1981).

<sup>6</sup>W. L. Johnson, P. Goalwin, and C. Cline, DOE Report CALT-822-122, 1980.

<sup>7</sup>P. Duwez, *Progress in Solid State Chemistry*, edited by H. Reiss (Pergamon, Oxford, 1966).

<sup>8</sup>W. L. Johnson and B. M. Clemens, invited contribution to Fall TMS-AIME Meeting, Sept. 1979, Milwaukee, Wis. (unpublished).

<sup>9</sup>A. M. Campbell and J. E. Evetts, *Adv. Phys.* **21**, 199 (1972).

<sup>10</sup>D. Dew-Hughes, *Philos. Mag.* **30**, 293 (1974).

<sup>11</sup>A. B. Pippard, *Philos. Mag.* **19**, 217 (1969).

<sup>12</sup>P. H. Kes and C. C. Tsuei, *Phys. Rev. Lett.* **47**, 1930 (1981).

<sup>13</sup>K. Yamafuji and F. Irie, *Phys. Lett.* **25 A**, 387 (1967).

<sup>14</sup>R. Labusch, *Cryst. Lattice Defects* **1**, 1 (1969).

<sup>15</sup>A. I. Larkin and Yu. N. Ovchinnikov, *J. Low Temp. Phys.* **34**, 409 (1979).

<sup>16</sup>J. Pearl, *J. Appl. Phys.* **37**, 4139 (1966).

<sup>17</sup>E. J. Kramer and A. Das Gupta, *Philos. Mag.* **26**, 769 (1972).

<sup>18</sup>A. Das Gupta and E. J. Kramer, *Philos. Mag.* **26**, 779 (1972).

<sup>19</sup>E. H. Brandt, *J. Low Temp. Phys.* **26**, 709 (1977).

<sup>20</sup>B. M. Clemens and W. L. Johnson (unpublished).